Delayed Encounter of Parental Genomes Can Lead to Aneuploidy in *Saccharomyces cerevisiae*

Alan Michael Tartakoff,[1] David Dulce, and Elizabeth Landis
Pathology Department and Cell Biology Program, Case Western Reserve University, Cleveland, Ohio 44106
ORCID ID: 0000-0002-8094-3345 (A.M.T.)

ABSTRACT We have investigated an extreme deviation from the norm of genome unification that occurs during mating in the yeast, *Saccharomyces cerevisiae*. This deviation is encountered when yeast that carry a mutation of the spindle pole body protein, Kar1, are mated with wildtype cells. In this case, nuclear fusion is delayed and the genotypes of a fraction of zygotic progeny suggest that chromosomes have "transferred" between the parental nuclei in zygotes. This classic, yet bizarre, occurrence is routinely used to generate aneuploid (disomic) yeast. [*kar1* × wt] zygotes, like [wt × wt] zygotes, initially have a single spindle pole body per nucleus. Unlike [wt × wt] zygotes, in [*kar1* × wt] zygotes, the number of spindle pole bodies per nucleus then can increase before nuclear fusion. When such nuclei fuse, the spindle pole bodies do not coalesce efficiently, and subsets of spindle pole bodies and centromeres can enter buds. The genotypes of corresponding biparental progeny show evidence of extensive haplotype-biased chromosome loss, and can also include heterotypic chromosomal markers. They thus allow rationalization of chromosome "transfer" as being due to an unanticipated yet plausible mechanism. Perturbation of the unification of genomes likely contributes to infertility in other organisms.

KEYWORDS karyogamy; *kar1*; aneuploidy; fertilization; *S. cerevisiae*

REGARDLESS of whether the nuclear envelope (NE) breaks down during mitosis, the integrity of centrosomes is essential for genomic stability. Integrity could be especially susceptible to disturbance during fertilization when two parental sets of chromosomes normally become unified. Nevertheless, there has been only limited investigation of lesions that destabilize genome unification. We are concerned with an example of such instability.

When haploid cells of *S. cerevisiae* are exposed to mating factor, a microtubule cable that is anchored to the spindle pole body (SPB) in the NE extends toward the tip of the mating projection. If a mating partner is adjacent and the cells fuse, the cables extending from each SPB exert a pulling force that causes the nuclei to congress. Nuclear contact is established within minutes at the SPB "half-bridge" where the Kar1 protein is anchored by its carboxy-terminus. After nuclear fusion (karyogamy) and merging of the two parental SPBs, the SPBs replicate, and the resulting zygote buds repeatedly, producing diploid progeny (Figure 1A) (Byers and Goetsch 1975; Muller 1985; Vallen *et al.* 1992; Spang *et al.* 1995; Melloy *et al.* 2007; Gibeaux *et al.* 2013).

Kar1 was first characterized using a selection to identify mutants that allow heterotypic exchange (cytoduction) of mitochondria when crossed with wild-type haploid cells (Conde and Fink 1976). [*kar1* × wt] crosses can also be used to exchange prions and killer virus, and to learn whether nuclear factors shuttle between nucleus and cytoplasm (Liu *et al.* 1996; Demeter *et al.* 2000; Chernoff *et al.* 2002; Wickner *et al.* 2007). Exchange can be attributed to the budding of haploid parental nuclei that include cytoplasmic components of mixed parental origin. Nevertheless, early studies of [*kar1* × wt] zygotes did also detect what appeared to be a modest amount of nuclear fusion (Conde and Fink 1976; Rose and Fink 1987).

Kar1 is required for mitotic growth, but growth appears normal when specific internal domains of Kar1 have been mutated or deleted, as in the original *kar1-1* mutant, and in the *kar1Δ15* mutant that we have studied. The phenotypes of both mutants are constitutive, not requiring a change of temperature. In [*kar1Δ15* × wt] zygotes, anchoring of cytoplasmic microtubules to the SPB is deficient (Figure 1A, lower image) and nuclear congression is slowed (Vallen *et al.* 1992; Gibeaux

doi: https://doi.org/10.1534/genetics.117.300289
Manuscript received September 13, 2017; accepted for publication October 31, 2017; published Early Online November 17, 2017.
Supplemental material is available online at www.genetics.org/lookup/suppl/doi:10.1534/genetics.117.300289/-/DC1.
[1]Corresponding author: Pathology Department, Wolstein Bldg., Case Western Reserve University, 2103 Cornell Rd., Cleveland, OH 44106. E-mail: amt10@case.edu

et al. 2013). Centriole duplication has been studied in detail in higher eukaryotes (Vallen *et al.* 1994; Nigg and Stearns 2011; Firat-Karalar and Stearns 2014; Nam *et al.* 2015), and Kar1 is required for SPB duplication (Vallen *et al.* 1994), but homologs of Kar1 are not known.

Curiously, in "exceptional cytoductant" progeny of [*kar1* × wt] crosses, elegant and thought-provoking experiments have shown that any of a number of chromosomes appear to have "transferred" from one parental nucleus to the other parental nucleus (Dutcher 1981). In fact, such protocols are routinely used to move chromosomes and plasmids between cells, *e.g.*, to construct disomic strains (Nilsson-Tillgren *et al.* 1980; Hugerat *et al.* 1994; Georgieva and Rothstein 2002; Torres *et al.* 2007). Possibly equivalent behavior has been observed in other situations, some of which could contribute to evolutionary diversification of yeasts (Elion *et al.* 1995; Morales and Dujon 2012).

Several features are characteristic of exceptional cytoductants: (a) "transfer" can occur both to and from the *kar1* parent, (b) "transfer" of two or more chromosomes occurs more frequently than expected if each event were independent of the other, (c) chromosomes remain intact, (d) strong haplotype bias can be detected, despite the presence of heterotypic chromosome(s) (Dutcher 1981; Hugerat *et al.* 1994; Torres *et al.* 2007).

Although the initial studies did not identify a mechanism of chromosome transfer, the production of exceptional cytoductants might involve the passage of a single parental nucleus into a bud, along with receipt of one or more chromosomes from the heterotypic parental nucleus. It is not clear, however, how such heterotypic chromosome(s) could gain access. Exceptional cytoductants are not diploid—judging from experiments with recessive drug-resistance markers—so the production of exceptional cytoductants has not generally been thought to require nuclear fusion. There is, however, no other reason to think that these progeny derive primarily from a single parental nucleus, rather than from nuclei that had fused.

As is discussed below, we find that "transfer" can be accounted for as being a consequence of fusion of parental nuclei followed by extensive chromosome loss. Especially from this point of view, there could be significant parallels between the mechanisms underlying chromosome "transfer" in yeast and the biology of cells of higher eukaryotes. This is despite the fact that yeast undergoes closed mitosis (*i.e.*, the NE does not break down) and the observation that the yeast genome remains tethered to SPBs during nearly all of the cell cycle (Loidl 2003; Kitamura *et al.* 2007). For example, classical methods for assigning genes to a single chromosome have often used experimental interspecies hybrids of human cells and cells of rodents. Since human chromosomes are preferentially lost from such hybrids, if an individual human chromosome is selected for, progressive losses ultimately can yield cell lines that include only a single heterotypic (human) chromosome—as in most yeast exceptional cytoductants (Kao and Puck 1970; Rao and Johnson 1972; Ruddle and Kucherlapati 1974; Walter and Goodfellow 1993). Mechanisms underlying the losses from these hybrid cells are not known. They could reflect incomplete or asynchronous genome unification or species-specific incompatibilties of centromere/kinetochore interactions. Moreover, the parental bias of loss could signify that the two contributing genomes retain some degree of spatial independence. This view is compatible with the observation that parental genomes normally remain spatially separate from each other during the initial cell divisions of mammalian zygotes (Mayer *et al.* 2000).

We have investigated the mechanisms that underlie apparent chromosome transfer among [*kar1* × wt] progeny since chromosome exit and entry through nuclear pores appear improbable, since strains with defined aneuploidies provide a valuable resource, and since insight into these events could aid in understanding aneuploidy in man.

The present observations emphasize the interest of studying genome unification during fertilization, as well as the consequences of inadvertent cell fusion or impaired cytokinesis, both of which can cause cells to have extra centrosomes (Duelli *et al.* 2007; Ganem *et al.* 2009; Vanneste *et al.* 2009; McNally and Anderson 2011; Maiato and Logarinho 2014; McCoy 2017). Unilateral lesions that affect genome unification would likely be incompatible with successful fertilization. The present study illustrates the magnitude of disruption that can be caused.

Materials and Methods

Cell culture

Cells were grown and studied in synthetic medium at 23°. Routine cultures included 2% glucose. To follow GFP-Esc1, cells in which transcription of GFP-Esc1 is under control of a galactose-inducible promoter were grown with 2% raffinose, shifted to 2% galactose for 2 hr, washed, and shifted to glucose medium before crossing.

Yeast strains

The strain and plasmid lists are Supplemental Material, Table S1 and Table S2. Standard yeast genetic procedures were used. The construction of strains used to estimate chromosome loss is described in the legend of Table S3.

To construct a *kar1Δ15/KAR1* diploid, a *kar1Δ15* haploid was transformed with a plasmid encoding wt *KAR1*. After crossing with a Kar1+ wt strain and selecting the diploid, the plasmid was counterselected with 5′-FOA.

Imaging

Cell mixtures were applied to the surface of 1.5%-agarose-CSM-glucose in multiwell plates. After appropriate periods of time, the cells were washed off and sedimented; 1 μl samples of the pellet were applied to 1.5% agarose pads on microscope slides including growth medium and 2% agarose (Zapanta Rinonos *et al.* 2012). They were examined in a Deltavision RT epifluorescence microscope with an automated stage (Applied Precision) and a 100× oil immersion objective (Olympus UPlanApo 100x/1.40; ∞/0.17/FN26.5). z-stacks were captured at 0.2–1 μm intervals using a CCD digital camera (Photometrics CoolSnap HQ). Out-of-focus light was removed using the Softworks deconvolution software (20 cycles) (Applied Precision). Complete through-focal series were examined in all cases.

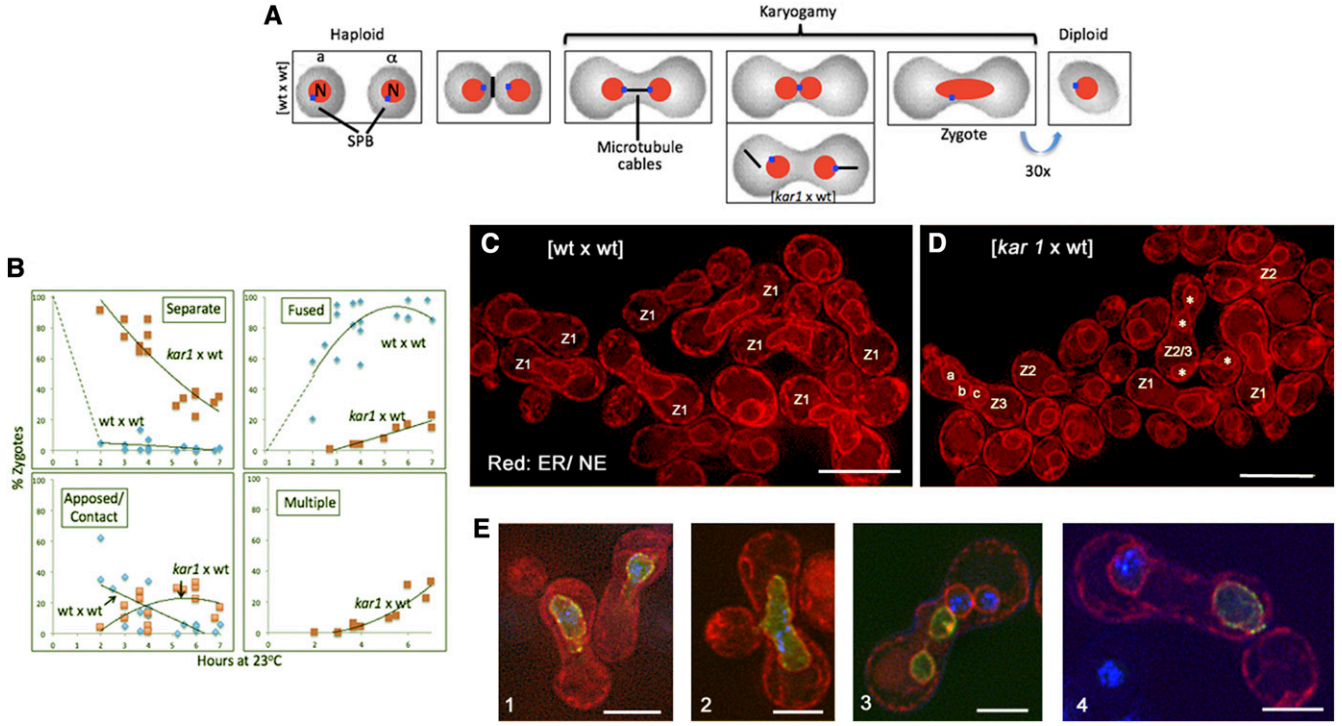

Figure 1 Overview of zygote formation. (A) Stages of zygote formation. The aligned sequence of six images schematizes the normal course of events. The single lower panel illustrates the impact of unilateral *kar1* mutations on the position of SPBs, and the orientation of cytoplasmic microtubule cables shortly after cell fusion (Rose and Fink 1987). As indicated, zygotes bud repeatedly (Muller 1985). (B) Kinetics of karyogamy. Wild-type strains were crossed. In parallel, the same MATa wt strain was crossed with an isogenic MATα *kar1* strain. The mating mixtures were fixed after increasing periods of time, and stained to detect DNA. Nuclei were classified for each zygote as being (1) separate and comparable in size to nuclei of haploid cells, (2) in contact with each other (for [wt × wt]) or apposed (for [*kar1* × wt]), (3) fused—meaning that there was a single larger DNA mass, or (4) multiple—meaning that there were more than two DNA masses. Note that karyogamy is delayed in the [*kar1* × wt] crosses, by comparison to [wt × wt] crosses. Data from four replicate experiments are included. Each symbol is the average of three independent samples from a single experiment; 100 zygotes were tabulated in each sample. The trend line, based on least squares, was calculated using Excel. Blue diamond symbols: [wt × wt] data. Orange square symbols: [*kar1* × wt] data. Note: In these experiments and all others, the *kar1* allele used was *kar1Δ15* (Vallen *et al.* 1992). Strains: ATY2111 × ATY2112 and ATY2111 × ATY4263. (C) Overview of zygote nuclei. Micrograph of [wt × wt] crosses conducted over 5 hr. Parental cells expressed mRFP-HDEL to mark the lumen of the ER/NE. Each zygote includes a single large nucleus (Z1). Bar, 8 μm. Strains: ATY7431 × ATY7266. (D) Overview of zygote nuclei. Micrograph of [*kar1* × wt] crosses conducted in parallel with (C). These zygotes can contain more than two nuclei (Z1, Z2, *etc.*), most of which are of the same size as the nuclei of haploid cells. The letters (a, b, c) are within three AN of one zygote. In the zygote labeled Z2/3, the two parental nuclei are dividing (asterisks), and one of the progeny nuclei has entered the bud. Bar, 8 μm. Strains: ATY7431 × ATY7191. (E) A wt cell was preinduced to produce GFP-Esc1 (to mark the inner aspect of the NE) and then was crossed for 3 hr with a *kar1* cell that expressed CFP-tagged lac repressor (lacI-CFP) and carried a high-copy plasmid with a lacO repeat. The two images at the left illustrate large nuclei that express both markers. In the two images at the right each nucleus expresses a single label. Note the ongoing division of one nucleus in (3), as is also illustrated in Figure S1. All parental cells expressed the ER/NE marker, mRFP-HDEL. B, bud; N, nucleus. Bar, 6 μm for (1–3) and 4 μm for (4). Strains: ATY6128 × ATY1550.

To stain DNA, growing cells were fixed for 1–5 min by addition of formaldehyde to 2%, washed in water, incubated for 5 min in 10 μg/ml Hoechst 33342, washed and examined using a DAPI filter.

We have seen no indication that SPBs labeled with Spc42-CFP are unstable or fragment.

Statistics

At least three independent experiments (biological replicates) were performed for all experiments.

Mating assays

Speed of congression and fusion: Equal volumes of actively growing cultures (OD_{600} = 1–2) were mixed, sedimented, resuspended in glucose-containing complete synthetic medium (CSM) and replicate 50 μl samples were applied to the surface of Petri dishes containing solid 2% agar-CSM-glucose. At the appropriate times, cells were washed off, fixed, and stained with Hoechst 33342. At least three fully independent experiments were performed in each case. Full data sets with Excel trend lines are illustrated. These lines are based on the method of least squares.

Loss of heterozygosity assays: Equal volumes of pairs of actively growing cultures (OD_{600} = 1–2) were mixed, sedimented, and resuspended in CSM-glucose at OD_{600} = 2; 50 μl samples were then applied to the surface of 1.5% agarose-CSM-glucose in multiwell dishes. After 8 hr at room temperature they were washed off, spread on CSM-glucose plates or plates lacking leucine and tryptophan, and allowed

Table 1 Number of nuclei and spindle pole bodies in zygotes

Parameter	T = 5 hr	T = 7.5 hr	Strains	
Zygotes with one large nucleus (%)	100[a]	100[a]	[wt × wt]	a
	13 ± 6.9	36 ± 1.1	[*kar1* × wt]	b
Zygotes with two nuclei (%)	0	0	[wt × wt]	c
	82 ± 8	54 ± 3	[*kar1* × wt]	d
Zygotes with three or more nuclei (%)	0	0	[wt × wt]	e
	3.8 ± 1.9	9.9 ± 1.3	[*kar1* × wt]	f
For zygotes with one large nucleus, number of SPBs per nucleus	1.6 ± 0.2	1.4 ± 0.1	[wt × wt]	g
	2.3 ± 0.2	2.7 ± 0.1	[*kar1* × wt]	h
For zygotes with two nuclei, number of SPBs per nucleus	NA[b]	NA	[wt × wt]	i
	1.47 ± 0.14	2.5 ± 0.16	[*kar1* × wt]	j
Zygotes with more than two SPBs (%)	0	0	[wt × wt]	k
	52.3 ± 17.7	62.7 ± 7.7	[*kar1* × wt]	l

In three independent experiments, a wt strain (ATY7058) was crossed with an isogenic wt strain (ATY7266) or an isogenic strain that carried the *kar1Δ15* mutation (ATY7191). After 5 and 7.5 hr, the mating mixtures were harvested, and zygotes were photographed by Deltavision microscopy, irrespective of whether they had buds; 34–55 zygotes were counted for each condition. All haploid parental strains expressed Spc42-CFP and mRFP-HDEL. All counts pertain to the body of zygotes, exclusive of buds. The numerical entries are averages ± SD.

[a] As shown in Figure 1C, essentially all [wt × wt] zygotes have a single nucleus.

[b] Not applicable since the parental nuclei in [wt × wt] zygotes fuse within 5 min after cell fusion.

to grow for 2–3 days at 30° before counting colonies. In certain cases, the plates included 3 μg/ml cycloheximide or 60 μg/ml canavanine (in which case they lacked arginine). To identify auxotrophic and drug-resistant characteristics of the colonies, 50 μl microcultures were established from single colonies in 96-well plates using media identical to the plates from which the colonies had been recovered. After overnight shaking, they were transferred to diagnostic plates lacking adenine, arginine, histidine, lysine, both phenylalanine and tyrosine, or uracil. They were also tested for growth in the presence of cycloheximide (3 μg/ml), canavanine (60 μg/ml) (on plates lacking arginine) or nourseothricin (0.1 mg/ml). To avoid the possible impact of jackpot occurrences, a total of 15 experiments were performed for each type of cross ([wt × wt] and [*kar1* × wt]) and the colony counts were pooled. The data summarized in Figure 6, D and E concern analysis of a total of >250 microcultures, each.

Data availability

Relevant data are provided either in the figures and tables, or in this *Materials and Methods* section. All yeast strains will be made public.

Results

Kinetics of karyogamy

To provide an overview of the normal progress of karyogamy, we prepared [wt × wt] mating mixtures, fixed them after 0–7 hr at room temperature, and then stained their DNA (Figure 1B). The half-time for appearance of a large single DNA mass in the resulting zygotes was 2–3 hr. Since such staining is characteristic of nuclei that have undergone karyogamy, we label such zygotes as "fused." In parallel [*kar1* × wt] crosses—although zygotes formed as rapidly as for [wt × wt] crosses—two or more DNA masses remained visible for several hours. These zygotes therefore are classified as having "separate" or "multiple" nuclei in the figure. The size of their nuclei was comparable to that of the nuclei of haploid cells. Zygotes with a single larger nucleus comparable to those of [wt × wt] zygotes began to appear only after a delay of ~3 hr. By 7.5 hr, about one-third of the [*kar1* × wt] zygotes had only a single large DNA mass. Figure 1B also tabulates the fraction of zygotes in which the DNA masses appeared to touch each other. In [wt × wt] zygotes, these were transient, and are labeled as "contacts." In [*kar1* × wt] zygotes, they often persisted for hours, and are designated as "apposed nuclei" (ANs). They are further discussed below.

To define the contour of the NE in zygotes, we followed a luminal marker of the ER and NE, mRFP-HDEL. In essentially all 5-hr [wt × wt] zygotes, rather than having nuclei whose diameter was comparable to the diameter of the nuclei of haploid cells, only a single larger nucleus was visible (Figure 1C and Table 1).

In parallel [*kar1* × wt] crosses, there was significant variety in the size and number of zygotic nuclei, which likely reflects the balance between their fusion and division, as well as ongoing budding. Figure 1D illustrates a field of cells after 5 hr. At this time most zygotes still had two nuclei ("Z2"), ~10% had more than two nuclei ("Z3") and zygotes with a single nucleus ("Z1") could be found. The presence of more than two nuclei per zygote is consistent with images of nuclear division within the body of the zygote, as shown in the zygote labeled "Z2/3," and in several panels in Figure S1 (see File S1 for supplementary figure legends). Especially the images in Figure 1E and Figure S1 show that two or more nuclei were often apposed to each other, reminiscent of observations of pronuclei in *Caenorhabditis elegans* (Audhya *et al.* 2007; Galy *et al.* 2008; Golden *et al.* 2009; Gorjanacz and Mattaj 2009; Rahman *et al.* 2015).

In [wt × wt] crosses, the large size of the zygote nucleus is expected to result from karyogamy. In [*kar1* × wt] zygotes, to document the origins of the large nuclei, we followed

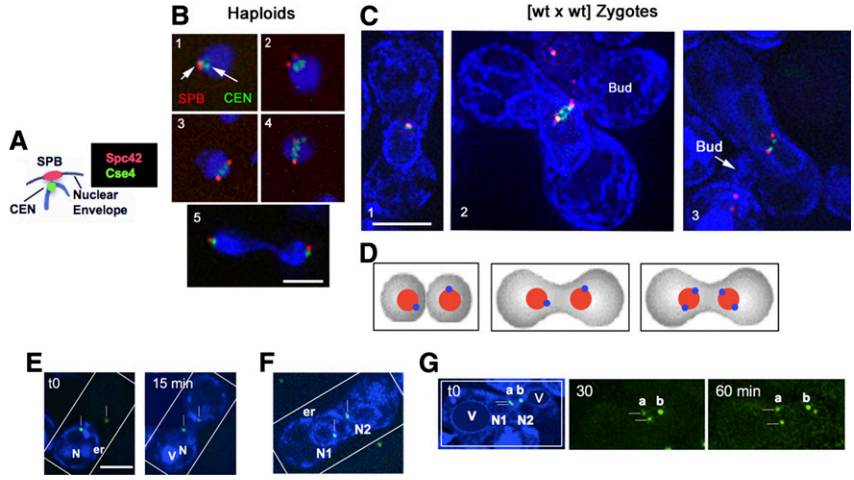

Figure 2 SPB duplication and migration in haploid cells and zygotes. (A) Diagram of the position of the SPB, nuclear envelope, and centromere clusters. (B) Cell cycle progression in wild-type haploid cells. Note (1) the single SPB (Spc42-CFP) and cluster of centromeres (Cse4-GFP) at the beginning of the cell cycle, (2) SPB duplication in parallel with the duplication of centromere clusters, (3 and 4) metaphase intermediates in which centromeres span between SPBs, and (5) telophase. Chromatin (Htb2-mRFP) is pseudocolored blue. Spc42-CFP is pseudocolored red. Cse4-GFP remains green. Bar, 5 μm for all panels of Figure 2. Strain: ATY3158. (C) Typical [wt × wt] 5-hr zygotes in which the SPB (Spc42-CFP, pseudocolored red) and CEN clusters (Cse4-GFP, green) progress from near-superposition (left) to metaphase (middle) and resolution (right). The ER/NE marker, mRFP-HDEL, is pseudocolored blue. Strains: ATY7431 × ATY7266. (D–G): early stages of SPB biology in [*kar1* × wt] zygotes. (D) Schematic of the observations included in (E–G). In (E–G), both parental cells expressed Spc42-CFP to label the SPBs, and the wt cells also expressed mRFP-HDEL to highlight the ER/NE. CFP is pseudocolored green and mRFP is pseudocolored blue. The letter (N) is positioned beneath nuclei. The prezygotes or zygotes of interest are enclosed by white rectangles. The SPBs are indicated by short white lines. The peripheral ER (er) and the vacuole (V) are also labeled. Strains: ATY7058 × ATY7160. (E) SPBs at the time of cell fusion. Crosses were initiated 3 hr before imaging. In the first image (t0) a single SPB was visible in both cells of the prezygote. Judging from the restriction of mRFP-HDEL to the cell on the lower left, fusion had not yet occurred; 15 min later, mRFP-HDEL was visible in both cells, implying that they had fused. Note that both parental SPBs remained separate after cell fusion. (F) Persistence of single parental SPBs in the separate nuclei of early zygotes. This zygote was imaged 3 hr after initiating the cross. The presence of two or more nuclei per [*kar1* × wt] zygote is also shown in Figure 1E and in Figure S1. (G) Visualization of the increase of the number of SPBs. Zygotes were imaged 3 hr after initiating a cross. Note in the first image (t0) that one SPB (a) had begun to double (the pair of foci is designated by two white lines). Over the following hour, it gave rise to two separate SPBs, and the second SPB (b) also began to do so. In the first panel (t0), the two bright blue vacuoles have been concealed to focus attention on the green SPB signals.

distinct markers of each of the two parental cell nuclei. Figure 1E (1 and 2) for example, illustrates large fused nuclei and 3 and 4 illustrate nuclei that had not undergone heterotypic fusion. For these experiments, the markers of the parental nuclei were either pulse-labeled GFP-Esc1 (Andrulis *et al.* 2002; Niepel *et al.* 2013), or a lacO-tagged high copy plasmid that was detected with lacI-CFP.

Characterization of apposed nuclei

Since the ANs might conceivably allow chromosome transfer, we characterized them further. The sites of contact between the NE of ANs did not necessarily coincide with the SPB (Figure S1H) or the nucleolus (Figure S1I). Most important, the apposed nuclear envelopes of ANs appeared to be intact, judging from the continuity of two membrane markers (Figure S1, J and K), as well as the increased intensity of a luminal marker (mRFP-HDEL) at points of contact (Figure S1, G and J). Had the nuclear envelopes fused, we would have expected a uniform intensity of this marker at these points. Although nuclear pores (Nup49-GFP) were generally present at the sites of contact of ANs, pores were not required, judging from the position of the sites of contact of ANs that form in crosses of *nup120Δ* strains in which pores cluster, leaving areas of the NE without pores (Aitchison *et al.* 1995; Heath *et al.* 1995) (Figure S1L).

Given the evidence of heterotypic nuclear fusion in [*kar1* × wt] zygotes, we asked whether fused nuclei could yield buds and progeny that are aneuploid, as in exceptional cytoductants. For this purpose we used both cytological approaches (Figure 2, Figure 3, and Figure 4) and genetic approaches (see below).

An increase of SPB number can precede karyogamy

To localize SPBs and centromeres, we observed zygotes that expressed both the tagged and functional SPB core protein, Spc42-CFP, and mRFP-HDEL, as well as a tagged form of the variant histone H3 that is characteristic of all centromeric nucleosomes (Cse4-GFP) (Keith and Fitzgerald-Hayes 2000). As for haploid cells (Figure 2, A and B), we observed that the SPB of early [wt × wt] zygotes duplicated and that one of the resulting SPBs then migrated to the opposite face of the nucleus (Figure 2C) prior to entry into the bud. Figure 2B (3 and 4) and Figure 2C (2) illustrate metaphase intermediates in which a centromere cluster spans two SPBs.

In [*kar1* × wt] crosses, as schematized in Figure 2D, both parental nuclei also had only a single SPB at the time of cell fusion. Moreover, the initially separate nuclei in early zygotes continued to have a single SPB. The number of SPBs per nucleus subsequently doubled in many zygotes. Figure 2, E–G illustrate representative experiments that document these events. Figure 2E shows the presence of only single SPBs per cell both before and after cell fusion. Figure 2F shows an example of 3 hr zygotes that still have two nuclei and only one SPB per nucleus. Figure 2G shows the apparent doubling of both such SPBs that occurs with time. A further example of a zygote with two nuclei in which the SPBs have already doubled is in Figure 3A.

To evaluate the number of nuclei per zygote (estimated by following mRFP-HDEL) and SPB number (estimated by

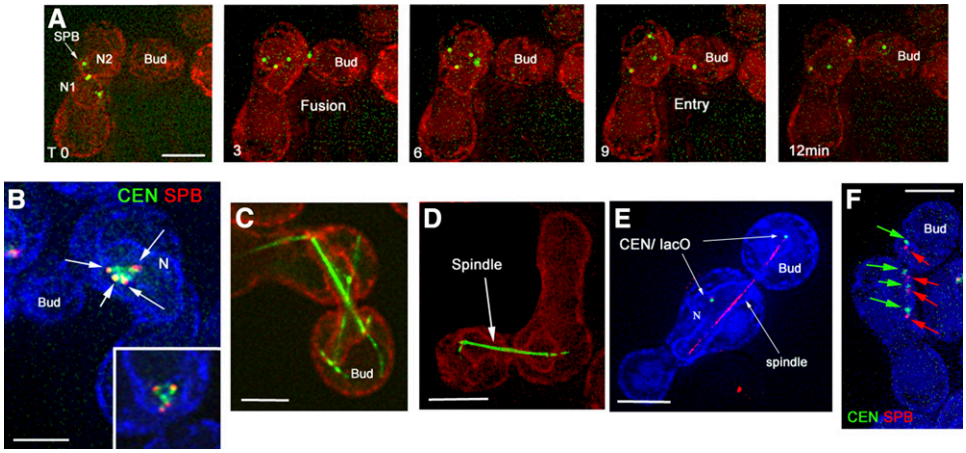

Figure 3 Aberrant behavior in [*kar1* × wt] zygotes, 5 hr crosses. (A) Time-lapse of fusion of two nuclei (N1 and N2) in a [*kar1* × wt] zygote. The first time point (t0) shows that each nucleus had two SPBs (Spc42-CFP) before fusion (one is shared at the site of imminent fusion). After fusion (t = 3 min), four SPBs were present in the nucleus. At the 9-min time-point, one SPB entered the bud. Spc42-CFP was pseudocolored green. The ER/NE was labeled with mRFP-HDEL (red). Bar, 5 μm for all panels of Figure 3. Strains: ATY7058 × ATY7160. (B) Supernumerary SPBs (Spc42-CFP; arrows) that cluster (arrows) along with centromeres (Cse4-GFP) in [*kar1* × wt] zygotes. A second example is in the inset. Since these images are projections of a through-focal series of z-planes, the SPBs are not always visible at the edge of the nucleus. Among 58 [*kar1* × wt] zygotes with a single large nucleus from three experiments, 20 had a cluster with more than two SPBs. Spc42-CFP is pseudocolored red. mRFP-HDEL is pseudocolored blue. Strains: ATY7431 × ATY7191. (C) Note the complex spindle labeled with Tub1-GFP in a [*kar1* × wt] zygote. Among 26 [*kar1* × wt] zygotes with a single large nucleus from three experiments, nine showed more than one spindle. Labels: mRFP-HDEL, Tub1-GFP. Strains: ATY7056 × ATY6616. (D) A typical single spindle in a [wt × wt] zygote. Labels: mRFP-HDEL, Tub1-GFP. Strains: ATY2000 and ATY7266. (E) In this [*kar1* × wt] zygote, note the spindle (red) with a lacO-tagged CEN at only one end, unlike wt haploid cells and zygotes in which loci distribute symmetrically at both ends of the spindle. Among 29 [*kar1* × wt] zygotes with a single large nucleus from three experiments, 10 showed aberrant positioning of the CEN foci relative to the spindle. Labels: mRFP-HDEL (pseudocolored blue), Tub1-CFP (pseudocolored red), lacI-GFP. Strains: ATY6922 × ATY7221. (F) Note the progression of paired SPBs (Spc42-CFP; red arrows) and CEN clusters (Cse4-GFP; green arrows) oriented toward the bud. Spc42-CFP is pseudocolored red. mRFP-HDEL is pseudocolored blue. Colored arrows indicate SPBs and centromeres. Among 58 [*kar1* × wt] zygotes with a single large nucleus and a bud (from three experiments), eight showed linear progressions oriented toward or entering the bud. In 65% of these zygotes, only one SPB was in the bud, as in this image. Strains: ATY7431 × ATY7191.

following Spc42-CFP) in both [wt × wt] and [*kar1* × wt] zygotes, we performed corresponding crosses that are summarized in Table 1. As expected, essentially all nuclei in [wt × wt] zygotes had undergone karyogamy at both time points (5 and 7.5 hr), the average number of SPBs per nucleus in these zygotes never exceeded 2.0, and no zygotes had more than two SPBs. By contrast, the percent of [*kar1* × wt] zygotes with a single large nucleus increased only gradually, reaching 36% by 7.5 hr. Among the [*kar1* × wt] zygotes with a single large nucleus, the average number of SPBs per nucleus exceeded 2.0 after both 5 and 7.5 hr. Among the zygotes with two nuclei, the average number of SPBs per nucleus exceeded 2.0 by 7.5 hr. Moreover, the number of SPBs per zygote exceeded 2.0 at both time points in the majority of zygotes. These numbers would presumably have been larger if SPBs were not concurrently "lost" to buds.

The presence of more than one SPB per nucleus in [*kar1* × wt] zygotes with two nuclei suggests that no checkpoint makes karyogamy a prerequisite for SPB doubling. Moreover, given the observation that zygotes can have multiple nuclei, no checkpoint restricts the number of nuclei to two.

When large nuclei do appear in [*kar1* × wt] zygotes, they appear to have been produced by a conventional mechanism, judging from a requirement for the membrane protein, Prm3, that is required for karyogamy in [wt × wt] zygotes (Figure S2, A–C) (Shen *et al.* 2009; Tartakoff and Jaiswal 2009). Moreover, as in [wt × wt] zygotes, karyogamy occurs at a site where parental SPBs contact each other (Figure 3A). Nevertheless, as we further discuss below, the SPBs often do not merge after karyogamy in [*kar1* × wt] zygotes. This discrepancy sets the stage for generation of aneuploid progeny by mechanisms distinct from those that have previously been identified for haploid yeast (Chan and Botstein 1993; Chial and Winey 1999; Yuen *et al.* 2007; Quevedo *et al.* 2015).

Sorting of spindle poles

To understand how a delay of karyogamy could lead to production of aneuploid progeny, we studied more closely the distribution and behavior of SPBs in [*kar1* × wt] zygotes that expressed Spc42-CFP. As shown in Figure 3A, when two nuclei in such a zygote fuse, the labeled SPBs remain separate, with only one SPB then entering the bud. Among 58 [*kar1* × wt] zygotes with a single large nucleus and a bud, five examples were found in which there was only one SPB in the bud.

Moreover, by 5 hr, it is not difficult to find clusters of four or more SPBs and centromeres within the body of the [*kar1* × wt] zygotes that have a single large nucleus (Figure 3B; 20/58 zygotes examined). Although not previously described in yeast, these structures are reminiscent of groupings of supernumerary centrosomes in human cells (Kleylein-Sohn *et al.* 2007). We suspect that kinetochore-SPB linkages are repeatedly tested at these sites, and that the spindle checkpoint is activated. Moreover, multiple spindles can be seen (Figure 3C; 9/26 zygotes examined), unlike [wt × wt] zygotes (Figure 3D). We also can find single lacO-tagged centromeric loci that do not segregate uniformly (Figure 3E; 10/29 zygotes examined).

In 5 hr [*kar1* × wt] zygotes, several SPBs can define a linear path toward, and extending into, the bud, with each

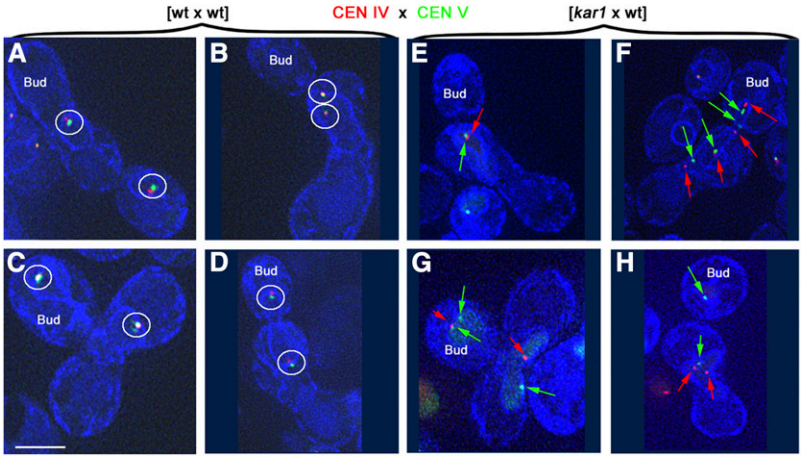

Figure 4 (A–H) Distribution of parental centromeres in fused nuclei of [wt × wt] and [*kar1* × wt] zygotes, 7 hr crosses. In each case, one parent expressed lacI-CFP to detect lacO repeats adjacent to CENIV, and the other parent expressed tetR-GFP to detect tetO repeats adjacent to CENV. The ER/NE was marked with mRFP-HDEL (pseudocolored blue). CFP is pseudocolored red. Bar, 5 μm for all panels of Figure 4. Left four panels, [wt × wt] zygotes. Note the pairing of colored loci (circles). Strains: ATY 7764 × ATY7691. Right four panels, [*kar1* × wt] zygotes. Distributions were much less uniform in [*kar1* × wt] zygotes than in [wt × wt] zygotes. Some appeared as for wildtype (E), but there were many examples of separation of centromeres. The pairs of loci in the bud in (F and G) could correspond to future diploid cells. The single green focus in the bud in (H) could correspond to a single genome. The cluster in the body of the zygote in (H) resembles the cluster of SPBs and centromeres in Figure 3B. The linear array in (F) resembles the linear array of SPBs and centromeres in Figure 3F. Among 51 [*kar1* × wt] zygotes with a single large nucleus and a bud (from five experiments), 14 had a single CEN locus in the bud (red or green); 23 had two or three visible CEN loci in the bud. The presence of only a single CEN color in the bud is consistent with inheritance of a single haplotype. When two or more CEN loci were in the bud, both colors were often present. N: Large single nuclei. Colored arrowheads mark the centromeres of distinct parental origin. Strains: ATY6829 × ATY7691.

SPB adjacent to, and presumably linked to, centromeres in cells that also express Cse4-GFP (Figure 3F; 8/58 examined). Perhaps most importantly, among these zygotes with a single large nucleus, we found that 66% had only a single SPB in the bud—as is also illustrated in Figure 3A—while 32% had two SPBs in the bud, and 2% had three SPBs in the bud. Entry of only a subset of SPBs into the bud provides an opportunity for delivery of only a subset of parental chromosomes to progeny.

Sorting of centromeres

To follow single chromosomes of distinct parental origin, we equipped each parental cell with one tagged centromeric locus that can be distinguished by color (CENIV-CFP and CENV-GFP). In [wt × wt] crosses of such strains examined after 7 hr, zygotes had one to two copies of each locus per large nucleus. When only one copy of each was present, and also when they had replicated, the CFP and GFP signals were invariably paired with each other (as designated by circles in Figure 4, A–D).

Among [*kar1* × wt] zygotes after 7 hr, paired red/green signals could also be found (Figure 4E); however, about half of [*kar1* × wt] zygotes did not show such pairing ($n = 80$ for zygotes with a single large nucleus with two to six visible CEN loci). In fact, a variety of distributions was found, as shown in Figure 4, F–H. Most interestingly, solitary loci could be found in the bud (Figure 4H), consistent the presence of a subset of SPBs (Figure 3, A and F) and genetic evidence of inheritance of a single haplotype (see below). For budded zygotes with a single large nucleus, and for which both colored loci were visible, we tabulated the presence of the loci in buds: 14/51 had only a single locus in the bud, and 23/51 had two to three loci in the bud.

Overview

Figure 5A presents a minimal model to account for the presence, sorting, and significance of supernumerary SPBs in [*kar1* × wt] zygotes, by comparison to [wt × wt] zygotes. The key observation is that SPBs double before nuclei fuse and that they can remain separate from each other after karyogamy. After karyogamy, in some cases only one SPB is present in the bud, suggesting that only a single haplotype will be delivered to progeny. Additionally, when multiple SPBs are present in one zygotic nucleus they can form a cluster. These units likely constitute a dead end. In the next section, we use an independent population-based approach to address the question of whether haplotype bias and aneuploid progeny can derive from nuclei that have fused.

Chromosome loss and haplotype-bias among biparental progeny

We have extended the cytological studies described above by following genetic markers that can report on the presence or absence of specific chromosomes. To focus on progeny of zygotes in which nuclei had fused, we equipped pairs of *leu2 trp1* mating partners with distinct plasmids, making it possible to restrict our attention to progeny that include both plasmids. The MATa parents (wt or *kar1*) carried a *TRP1* high copy (2μ) plasmid, while the 2μ plasmid in the MATα parent encoded Leu2 (Figure 6A). As expected, high copy plasmids can be found throughout the nucleoplasm of single large nuclei in [*kar1* × wt] zygotes and can access buds (Figure 6B). We refer to zygotic nuclei that include plasmid markers from both parents as being "biparental" and we refer to corresponding progeny as "biparental progeny." Since 2μ plasmids lack centromeres, this strategy to recover biparental progeny does not presuppose that centromere linkage of markers is accurate. All experiments described below include such 2μ plasmids. Additionally, the MATa parental cells (wt, *kar1*) carried recessive drug resistance mutations (*can1-100* and $cyh2^{Q37E}$). This made it possible to detect any loss of wild-type copies of the corresponding chromosomes (Vα, VIIα) among progeny by screening for resistance to canavanine or

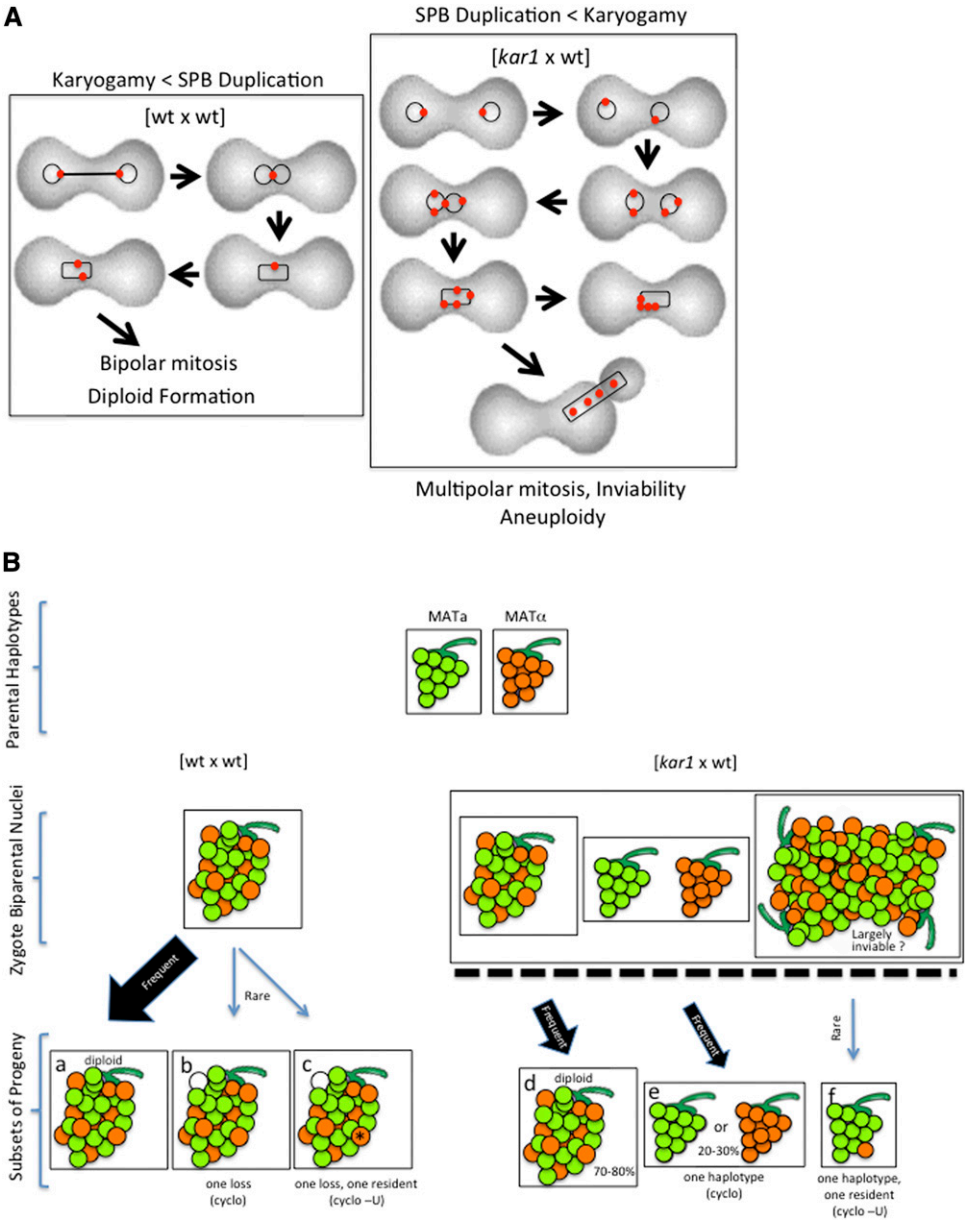

Figure 5 Schematic models to account for aneuploidy. (A) Number and fate of SPBs. Left: In [wt × wt] crosses, after cell fusion the two nuclei congress within minutes, due to the microtubule cable(s) that links the two SPBs (red). As a result, the two SPBs establish contact to form a single unit. They subsequently replicate in parallel with DNA replication. Right: In [*kar1* × wt] crosses, congression is slow, and the SPBs can replicate before karyogamy. When karyogamy occurs, contributing nuclei therefore can already have two SPBs. In such cases, the fused nucleus will have four SPBs that do not obligatorily fuse with each other. In some cases, only one enters the bud. Multiple SPBs can also cluster. (B) Genetic consequences. Top: Parental haploid strains whose centromeres are distinguished by color. Note that each has an equal number of centromeres (circles), all of which are linked to the SPB (stem). Left: [wt × wt] crosses. After karyogamy and SPB coalescence, all centromeres associate with the SPB of the biparental nuclei. The overwhelmingly predominant progeny in this situation are diploid (lower panel a). Other subsets of progeny can be selected for, *e.g.*, by including cycloheximide (cyclo), to select against one chromosome [open circle in (b)]. It is not linked to other centromeres from the same haplotype. (c) illustrates the outcome when inclusion of cycloheximide mandates loss of one chromosome (VIIα), and omission of uracil (–U) mandates retention of a different chromosome from the same parent (*) Right: [*kar1* × wt] crosses. After karyogamy—second row—we envisage three outcomes for the biparental zygote nuclei: (left) SPB fusion and unification of the two parental haplotypes, (middle) persistence of both separate SPBs with associated centromeres, or (right) accretion of multiple SPBs and their associated centromeres as clusters. The heavy dashed horizontal line indicates that only very few viable progeny are then produced. Judging from the observation that ~10–15% of all Leu+ Trp+ progeny resist cycloheximide or canavanine (Table 2), and lack the other MATα markers that we have tested, (Figure 6E)—and the anticipated parallel losses of MATa markers (in other zygotes)—we estimate that 70–80% of all viable progeny retain both parental haplotypes (option d). The second most likely outcome (option e: 20–30%) involves loss of one (or the other) entire parental haplotype. Rare outcomes (options f) could accompany loss of all but one chromosome of one parental haplotype. Such events can account for the classic observations of chromosome "transfer." Since different single heterotypic chromosomes can be selected for, these options illustrate the genetic mosaicism of outcomes. The 20–30% and 70–80% breakdown is based on data from Table 2. In fact, parallel preliminary experiments based on use of α-aminoadipate allow one to select against Lys+ and detect selective loss of multiple markers from the MATa haplotype.

to cycloheximide. Table S3 lists the additional genetic markers that were present.

When [wt × wt] and [*kar1* × wt] crosses were harvested after 8 hr (or 8 hr followed by 16 hr in liquid culture), and the mating mixtures were then spread on plates with rich medium (CSM-glucose), comparable numbers of colonies formed for both types of crosses. On plates lacking leucine and tryptophan; however, the yield of colonies was reduced by two orders of magnitude in [*kar1* × wt] crosses (Table 2). This reduction could reflect both the relative inefficiency of nuclear fusion and aberrant chromosome assortment after nuclear fusion. Experiments designed to estimate the relative fraction of progeny that have an unfused haploid parental nucleus do indicate that biparental progeny are a minority (Figure S3).

We compared colony size among progeny of [wt × wt] crosses and [*kar1* × wt] crosses (Figure 6C), as well as drug resistance characteristics. For [wt × wt] progeny, colony size

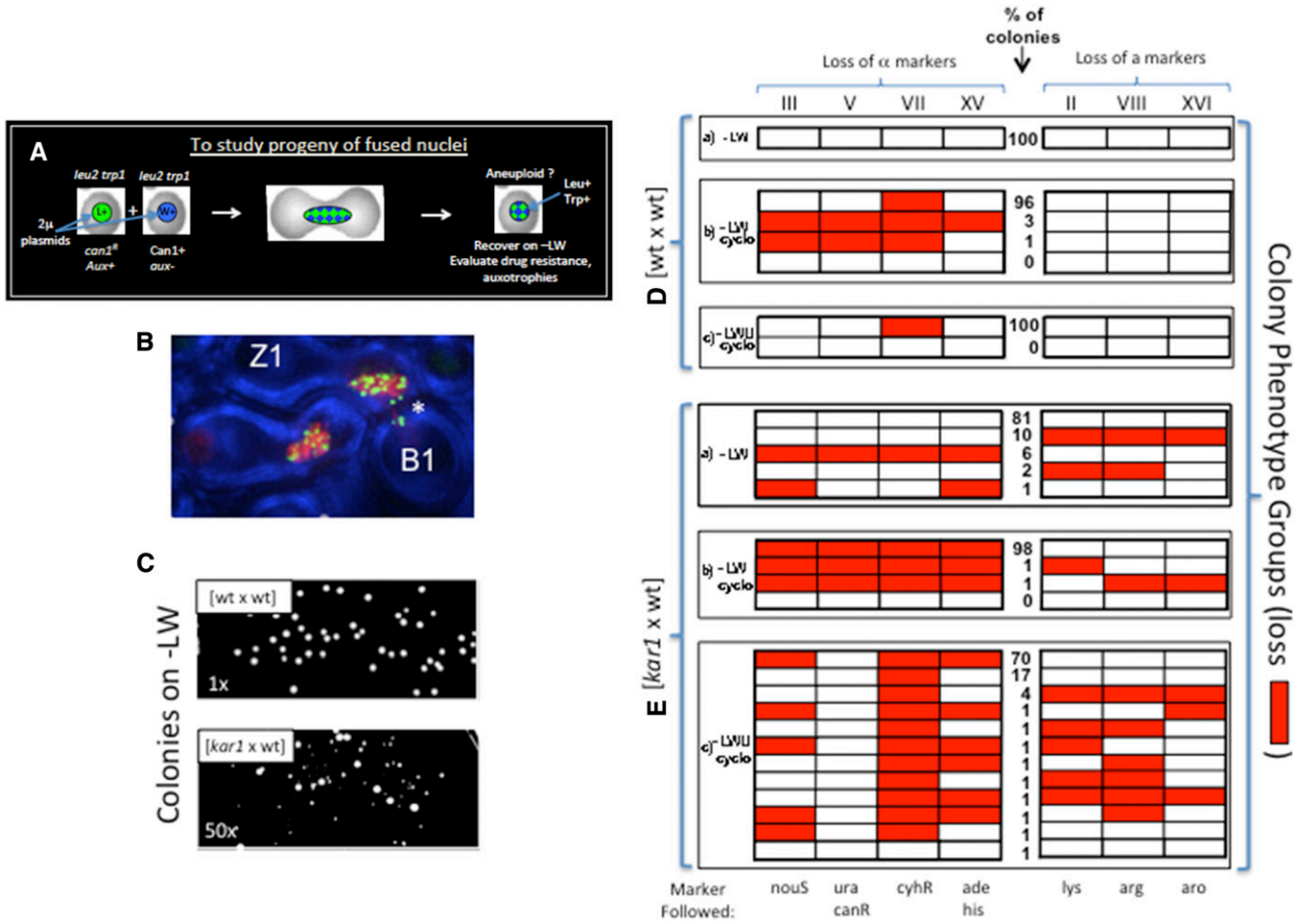

Figure 6 Strategy and observations to estimate marker losses. (A) Recovery of biparental progeny. Each parental cell carried *leu2* and *trp1* mutations. MATa strains (wt and *kar1Δ15*) carried a 2μ plasmid encoding Leu2, and the recessive mutations *can1-100* and *cyh2*^{Q37E}. The MATα strain carried a 2μ plasmid endcoding Trp1. These plasmids lack centromeres and their inheritance therefore does not depend on anchorage to microtubules. Several distinctive auxotrophies were also present (Table S3). Biparental progeny were recovered on plates lacking leucine and tryptophan. (B) Visualization of a 2μ plasmid carrying a lacO repeat in 5 hr [*kar1* × wt] zygotes in which the nuclei have fused. The nuclei were labeled with Htb2-mRFP and expressed lacI-GFP. For the horizontally oriented zygote at the top (Z1), note that multiple GFP-positive foci are distributed throughout the nucleus, and that these foci, as well as the red histone label, are entering its bud (B1) toward the lower right. The bud neck is indicated with an asterisk. A second unbudded zygote is at the bottom in the same field. Strains: ATY6176 and ATY6155. (C) Colony size of biparental progeny of [*kar1* × wt] crosses. Two 8 hr crosses were conducted: [wt × wt] (upper) and [*kar1* × wt] (lower). Mating mixtures were spread on doubly selective plates (–LW). Note the homogeneity of the [wt × wt] progeny and the heterogeneity of the [*kar1* × wt] progeny (plated at 50× higher concentration). Strains: MATa: ATY7498 (wt) and ATY7510 (*kar1*). MATα: ATY7451. (D and E) Estimation of marker loss (Colony Phenotypes). [wt × wt] and [*kar1* × wt] crosses were conducted for 8 hr followed by reincubation in doubly selective (–LW) medium for 16 hr. The mating mixtures were then spread on three types of plates: –LW, –LW with cycloheximide, or –LW with cycloheximide and lacking uracil. Colonies from 15 experiments were grown overnight, and then pinned onto diagnostic plates to monitor the presence of markers that distinguish the two parental haplotypes (Table S3). This involved evaluation of growth in the absence of uracil, adenine, histidine, lysine, arginine, or tyrosine and phenylalanine (aro), as well as growth in the presence of nourseothricin (nouS), cycloheximide (cyhR), or canavanine (canR). The numerical entries in the middle column indicate the percent of colonies that showed one or more characteristic set of losses (or no losses). For each panel, ≥250 colonies were analyzed. In the symbolic representation, losses are designated in red. (D) [wt × wt crosses]. Without marker-specific selection, <1% of colonies showed marker loss (Da). When cycloheximide was present (Db), there was only a slight tendency (<5% of colonies) to lose multiple markers. Interestingly, linkage was nevertheless evident for these colonies. The simultaneous absence of uracil further reduced the coordinate loss of multiple markers (Dc). (E) [*kar1* × wt] crosses. Without marker-specific selection (a), >80% of biparental colonies show no evidence of marker loss, and therefore are likely to be diploid. Nevertheless, loss is profound and the losses show strong haplotype bias. For example ~10% of colonies collected on –LW plates (a) lack all three MATa markers, but none from MATα; and a similar number (~6%) lack all four MATα markers, but none from the MATa haplotype. Among cycloheximide-resistant colonies (b), there were many examples of concordance of auxotrophies or drug-resistance characteristics. Thus, 98% of colonies that grew on –LW cycloheximide plates lacked all markers from the MATα haplotype (as expected upon loss of IIIα, Vα, VIIα and XVα). Moreover, these colonies were Arg+, Lys+, Phe+, and Tyr+. Since these latter markers were on chromosomes contributed by the MATa parent [II (*LYS2*), VIII (*ARG1*), and XVI (*ARO7*)], the progeny appear to have retained these chromosomes from the MATa haplotype. When the selection was on –LW canavanine plates, instead of –LW cycloheximide, we again observed comparable bias toward loss of markers from the MATα parental haplotype. Reciprocal haplotype enrichment can be achieved by using α-aminoadipate to select against MATa cells that were Lys+. A possible source of exceptional cytoductants. Despite the haplotype-specific concordance of marker loss for biparental [*kar1* × wt] progeny, haplotype uniformity is not absolute. For example, as tabulated in (c) for the [*kar1* × wt] outcomes,

was nearly uniform on plates lacking leucine and tryptophan (–LW), and resistance to canavanine or cycloheximide was rare ($\sim 10^{-5}$). By contrast, colonies derived from [*kar1* × wt] crosses were of variable size. Moreover, by comparison to [wt × wt] crosses, the incidence of apparent chromosome loss among biparental progeny of [*kar1* × wt] crosses increased by four orders of magnitude. Thus, by comparison to the number of colonies on –LW plates, 10–15% also resisted canavanine (15 ± 3%; $n = 3$) or cycloheximide (10 ± 5%; $n = 3$) (Table 2). Moreover, >90% of the canavanine-resistant colonies were also *ura*–. Since both *CAN1* and *URA3* are on chromosome Vα this concordance of phenotype strongly suggests that chromosome Vα was no longer present.

To study the genotypes of progeny with greater precision, single colonies were recovered from three types of plates. Type (a) plates simply lacked leucine and tryptophan (–LW). Type (b) plates also included cycloheximide, and type (c) plates—in addition to including cycloheximide—lacked uracil. Colonies from each type of plate (from a total of 15 experiments) were then analyzed on diagnostic plates that were designed to monitor loss of heterozygosity at nine loci corresponding to seven chromosomes (II, III, V, VII, VIII, XV, and XVI). The complementary auxotrophies and drug-resistance characteristics of the parental strains had been designed to make this possible (Table S3). Figure 6D presents the data for [wt × wt] crosses and Figure 6E presents the data for [*kar1* × wt] crosses, with the red color designating marker loss.

The analysis of biparental progeny of [wt × wt] crosses recovered on –LW plates showed that marker loss was rare (Figure 6Da). Moreover, of the subset of progeny on –LW plates that also resisted cycloheximide (Figure 6Db), 96% did not lose markers of other chromosomes. Only 3% concurrently lacked all other markers of the MATα haplotype. This frequency dropped to zero if a double selection was imposed, adding cycloheximide and removing uracil to select for retention of the *URA3* locus on chromosome Vα (Figure 6Dc).

Losses among [*kar1* × wt] progeny were much more frequent and were strikingly haplotype-specific for colonies recovered on –LW plates. Either parental haplotype could be favored with approximately equal frequency (6–10%) (Figure 6Ea). When cycloheximide was included to select for loss of chromosome VIIα, 98% of colonies showed concurrent losses of all markers from the same haplotype (Figure 6Eb). This seems likely to reflect the presence of centromeres from a single haplotype in zygotic buds, as suggested by the images in Figure 4.

In fact, parallel preliminary experiments based on use of α-aminoadipate allow one to select against Lys+, and detect selective loss of multiple markers from the MAT**a** haplotype. The inclusive estimates of the frequency of chromosome loss among biparental progeny therefore should be doubled to 20–30%. Figure 6Ec and Table 2 also show that, by selecting for loss of a marker from both parental haplotypes (*i.e.*, adding cycloheximide and omitting uracil), it is possible to recover progeny of mixed genotype, as for exceptional cytoductants.

When the original studies of chromosome "transfer" were performed, recessive markers were used to exclude diploid progeny (Dutcher 1981). Consideration was not given to the possibility that any concomitant loss of the very chromosomes that carried wildtype alleles of the recessive markers would have rendered cells resistant to the drugs in question. Drug resistance excludes true diploids. It does not exclude hypodiploid progeny in which loss of specific chromosomes occurred.

The impact of the *kar1* mutation on the genotypes of zygotic progeny would be affected by any widespread genetic instability during mitotic growth. In fact, we observed that the *kar1* mutation had little effect on genetic stability during mitotic growth. For example, *CEN* plasmids (*e.g.*, pRS316) were of comparable stability in *kar1* haploid cells and in wt during mitotic growth. Moreover, judging from use of recessive markers (*can*1-100, *cyh2*), chromosomal stability in *kar1*/wt diploids is comparable to that of wt/wt diploids.

Overview

Figure 5B summarizes the genetic characteristics of biparental progeny of [wt × wt] zygotes, by comparison to the biparental progeny of [*kar1* × wt] zygotes. Thus, in [wt × wt] crosses, after karyogamy and SPB coalescence, essentially all centromeres associate with the diploid SPBs of the biparental nuclei. The overwhelmingly predominant progeny therefore are diploid. Other subsets of progeny can nevertheless be selected for, *e.g.*, by including cycloheximide. In such cases, only a small fraction show haplotype linkage for marker loss, as expected if distinct subgroupings of parental centromeres are rare.

Judging from the observation that 10–15% of all biparental [*kar1* × wt] progeny resist cycloheximide or canavanine (Table 2), and lack all other MATα markers that we have tested (Figure 6E), we estimate that 70–80% of all viable biparental [*kar1* × wt] progeny retain both parental

we could select a subset of Leu+Trp+ cycloheximide-resistant progeny that retained a marker from the MATα parent: *URA3* (chromosome Vα). This was achieved by omitting uracil from the –LW cycloheximide selection plates. By omitting additional nutrients, one can recover a spectrum of strains that include other corresponding MATα markers, as in exceptional cytoductants. The Ura+ cycloheximide-resistant colonies recovered from [*kar1* × wt] crosses are 100- to 1000-fold less numerous than colonies recovered on –LW cycloheximide plates that included uracil (Table 2). This differential reflects the strength of the haplotype bias that is characteristic of such crosses, and likely reflects persistent centromere linkage to the SPB. In equivalent [wt × wt] crosses, progeny that survive in the presence of cycloheximide are recovered with a comparable very low frequency ± the additional requirement for uracil prototrophy (D, c; Table 2). We conclude that the haplotype-bias of chromosome loss among biparental [*kar1* × wt] progeny is incomplete, and the deviations from haplotype-bias should be considered a possible source of exceptional cytoductants. The protocols originally used to recover exceptional cytoductants, however, did not make it possible to know whether their production required karyogamy.

Table 2 Yield of successive subsets of progeny

Cross	As fraction of colonies on:	–LW	–LWR * Can	–LW Cyclo	–LWU Cyclo	1
[wt × wt]	CSM-glucose	0.62 ± 0.11				2
[*kar1* × wt]		5.4 ± 0.2 × 10^{-3} [3 × 10^{-3}]				3
[wt × wt]	–LW		3.3 ± 2.0 × 10^{-5}	1.4 ± 1.1 × 10^{-5}		4
[*kar1* × wt]			0.15 ± 0.03	0.1 ± 0.53 [0.1]		5
[wt × wt]	–LW cycloheximide				∼1 [0.9]	6
[*kar1* × wt]					2.8 × 10^{-2} – 4.4 × 10^{-3} [3–5 × 10^{-3}]	7
a	b	c	d	e	f	

At the end of the 8 hr crosses (4–5 biological replicates), cells were spread on the types of plates indicated in row (1). The yield of colonies was then estimated after 1–2 D at 30°; 200 colonies were analyzed for each experiment. Averages ± SD. were calculated. The data in square brackets were obtained from 8 + 16 hr protocols. Explanation: Entries in column c (rows 2 and 3), indicate the fraction of colonies recovered on –LW plates divided by the number recovered on CSM-glucose plates. In column d (rows 4 and 5), entries indicate the number recovered on –LW canavanine plates divided by the number recovered on –LW plates, *etc*. Our estimates of the frequency of inclusion of a heterotypic chromosome are comparable to Dutcher's. In Dutcher's studies, the estimates were relative to the total number of viable cytoductants. Our point of reference is, instead, the number of progeny that carry both parental high copy plasmids. Dutcher never specifies the duration of the crosses that she performed, so it is not possible to make an accurate comparison; however, assuming that the duration was comparable to ours, our normalization (to Leu+ Trp+ colonies) would be expected to yield somewhat fewer total viable zygotes, *i.e.*, presumably not all dinuclear zygotes undergo karyogamy and yield viable progeny. Moreover, her estimate of transfer frequency included a further adjustment since she was taking into consideration the chance of the recipient nucleus acquiring a chromosome that had been lost from a donor nucleus. Dutcher's text says "the frequency with which various nuclear markers were transferred varied ... from 0.7 to 19.5 exceptional transductants per 10,000 transductants examined." This is 0.1–2 × 10^{-3}. The Table above estimates our frequency of chromosome loss to be 10–15%, and the relative frequency of concurrent inclusion of one heterotypic marker to be 0.44–2.8 × 10^{-2} (*i.e.*, ∼1.6 × 10^{-2}). So, the present estimate of overall frequency of the equivalent of transfer is similar to Dutcher's, *i.e.*, ∼1.6 × 10^{-3}. Can, canavanine; Cyclo, cycloheximide

haplotypes, presumably as a reflection of delayed but ultimately accurate SPB coalescence. Nevertheless, the second most likely outcome involves loss of one (or the other) entire parental haplotype—as would be expected if indeed only a single chromosome complement had entered the bud, as depicted in Figure 5A. The still less frequent (rare) outcomes could reflect concomitant entry into the bud of one (or more) chromosomes of the second parental haplotype. As described in the legend of Table 2, the frequency of these outcomes is comparable to the frequency of exceptional cytoductants described by Dutcher. Length-dependence of entry of heterotypic chromosomes into the bud could account for Dutcher's observations that short chromosomes appear to transfer more frequently than longer chromosomes (Dutcher 1981).

Discussion

Nondisjunction during gametogenesis is widely considered to be a major contributor to genome instability during fertilization (Nagaoka *et al.* 2012; McCoy 2017). Accurate gamete fusion and unification of parental chromosome sets in zygotes are also essential for genetic stability. For example, chromosome loss could result from lesions that affect centrosome reorganization, or the alignment and anchoring of gamete-specific sets of chromosomes on the composite mitotic spindle, as upon inactivation of PLK-1 in *C. elegans* (Rahman *et al.* 2015). Nevertheless, during zygote formation in higher organisms, the potential danger of generating extra centrosomes during gametogenesis may be reduced by eliminating parental centrosomes (Manandhar *et al.* 2005). For example, human oocyte spindles assemble in the absence of centrosomes and a microtubule organizing center (Holubcova *et al.* 2015).

It is difficult to estimate the frequency with which aberrant genome unification may limit fertility. If the consequences are indeed severe, conventional means of diagnosing causes of aneuploidy that rely on analysis of the conceptus would be unable to detect these events. As examples of impaired anchoring of centromeres, mutation of a kinetochore-associated kinase (BUB1R), or a kinetochore protein in man (CEP57), results in mosaic variegated aneuploidy (Lebedev 2011; Snape *et al.* 2011; Vitre and Cleveland 2012).

In yeast, the microtubule cables that connect nuclei in [wt × wt] zygotes are responsible for congression of nuclei, and ultimately ensure alignment of the parental SPBs. These events are delayed in [*kar1* × wt] zygotes, allowing SPB number to increase prior to karyogamy. Moreover, since the parental SPBs do not obligatorily coalesce when these nuclei do fuse, biparental zygotic nuclei can have more than two SPBs, and, in these zygotes, one can readily find single SPBs and single centromeres that have entered into the bud. The SPBs in the bud seem likely to continue to associate with a single haplotype-specific complement of chromosomes, and thereby account for the haplotype bias of many biparental progeny. (We have attempted to define the parental origin of SPBs using an inducible construct to express tagged Spc42; however, the construct used—although previously used by others—is prohibitively leaky.) One or more heterotypic chromosomes from the body of the zygote—if released from SPB linkage—could secondarily become anchored to the SPB that enters the bud. Such events could account for the classic observations of chromosome "transfer" and the genetic mosaicism of progeny. If chromosomes associated with the centromeric loci in the body of the zygote did not enter the bud, they would be "lost," at least for the first cycle of budding. If indeed fused zygotic nuclei are intermediates in the production of exceptional cytoductants, one might predict several of their characteristics: (a) the lack of directionality of transfer, (b) the relatively

high frequency of double or triple transfers, and (c) chromosome integrity after transfer.

Other mechanisms might also contribute to haplotype bias and generation of exceptional cytoductants. Thus, progeny could include a single parental nucleus or a descendent of such a nucleus that has entered a bud. It remains unclear, however, how heterotypic chromosomes and 2μ plasmids would gain access to these progeny.

One possibility is that AN undergo some sort of transient fusion (Alabi and Tsien 2013) that allows 2μ plasmids and occasional chromosomes to transfer between nuclei, only one of which then enters a bud. Nevertheless, we have seen no indication that the integrity of the nuclear envelope is compromised at the points of nuclear apposition. Moreover, we performed [*kar1* × wt] crosses in which the nucleus of one parent was equipped with a 2μ plasmid carrying a lacO-tagged plasmid and lacI-GFP, while the other parent expressed Htb2-mRFP. Upon examining hundreds of ANs in zygotes derived from these parents, we found no evidence of frequent redistribution of this locus. The experiment presented in Figure S3 also implies that any transfer of 2μ plasmids must be rare. A further alternative explanation might involve occasional encapsulation of selected chromosomes in micronuclei that fuse with conventional nuclei. Such events are known in cells that accomplish open mitosis (Crasta *et al.* 2012; Hatch *et al.* 2013), but have not been described in yeast.

Fused biparental nuclei of [*kar1* × wt] zygotes transiently constitute an environment in which—although both parental genomes are present—each chromosome complement can segregate independently of the other. In addition to making it possible to select for designer genotypes, this environment could be valuable (a) to expose a genome temporarily to covalent modifications characteristic of a mating partner, or (b) to cause targeted *in vivo* chromosomal rearrangements, *e.g.*, between chromosomes contributed by each parent.

Acknowledgments

Thanks for materials to C. Antony, R. Baker, J. Cooper, N. Dean, V. Doye, S. Gasser, W.-K. Huh, M. Jayaram, J. Kilmartin, T. Lithgow, M. Rose, R. Rothstein, K. Runge, A. Straight, and R. Sternglanz. Thanks to P. Gruber, G. V. Boerner, D. MacDonald, M. Sy, and H. Worman for practical help and comments, and to D. Gitiforooz for help with the figures. Thanks to the National Institutes of Health (NIH) for R01GM089872 and P30CA43703-12, and thanks to the Visconsi family for support.

Literature Cited

Aitchison, J. D., G. Blobel, and M. P. Rout, 1995 Nup120p: a yeast nucleoporin required for NPC distribution and mRNA transport. J. Cell Biol. 131: 1659–1675.

Alabi, A. A., and R. W. Tsien, 2013 Perspectives on kiss-and-run: role in exocytosis, endocytosis, and neurotransmission. Annu. Rev. Physiol. 75: 393–422.

Andrulis, E. D., D. C. Zappulla, A. Ansari, S. Perrod, C. V. Laiosa *et al.*, 2002 Esc1, a nuclear periphery protein required for Sir4-based plasmid anchoring and partitioning. Mol. Cell. Biol. 22: 8292–8301.

Audhya, A., A. Desai, and K. Oegema, 2007 A role for Rab5 in structuring the endoplasmic reticulum. J. Cell Biol. 178: 43–56.

Byers, B., and L. Goetsch, 1975 Behavior of spindles and spindle plaques in the cell cycle and conjugation of Saccharomyces cerevisiae. J. Bacteriol. 124: 511–523.

Chan, C. S., and D. Botstein, 1993 Isolation and characterization of chromosome-gain and increase-in-ploidy mutants in yeast. Genetics 135: 677–691.

Chernoff, Y. O., S. M. Uptain, and S. L. Lindquist, 2002 Analysis of prion factors in yeast. Methods Enzymol. 351: 499–538.

Chial, H. J., and M. Winey, 1999 Mechanisms of genetic instability revealed by analysis of yeast spindle pole body duplication. Biol. Cell 91: 439–450.

Conde, J., and G. R. Fink, 1976 A mutant of Saccharomyces cerevisiae defective for nuclear fusion. Proc. Natl. Acad. Sci. USA 73: 3651–3655.

Crasta, K., N. J. Ganem, R. Dagher, A. B. Lantermann, E. V. Ivanova *et al.*, 2012 DNA breaks and chromosome pulverization from errors in mitosis. Nature 482: 53–58.

Demeter, J., S. E. Lee, J. E. Haber, and T. Stearns, 2000 The DNA damage checkpoint signal in budding yeast is nuclear limited. Mol. Cell 6: 487–492.

Duelli, D. M., H. M. Padilla-Nash, D. Berman, K. M. Murphy, T. Ried *et al.*, 2007 A virus causes cancer by inducing massive chromosomal instability through cell fusion. Curr. Biol. 17: 431–437.

Dutcher, S. K., 1981 Internuclear transfer of genetic information in kar1–1/KAR1 heterokaryons in Saccharomyces cerevisiae. Mol. Cell. Biol. 1: 245–253.

Elion, E. A., J. Trueheart, and G. R. Fink, 1995 Fus2 localizes near the site of cell fusion and is required for both cell fusion and nuclear alignment during zygote formation. J. Cell Biol. 130: 1283–1296.

Firat-Karalar, E. N., and T. Stearns, 2014 The centriole duplication cycle. Philos. Trans. R. Soc. Lond. B Biol. Sci. 369: 20130460.

Galy, V., W. Antonin, A. Jaedicke, M. Sachse, R. Santarella *et al.*, 2008 A role for gp210 in mitotic nuclear-envelope breakdown. J. Cell Sci. 121: 317–328.

Ganem, N. J., S. A. Godinho, and D. Pellman, 2009 A mechanism linking extra centrosomes to chromosomal instability. Nature 460: 278–282.

Georgieva, B., and R. Rothstein, 2002 Kar-mediated plasmid transfer between yeast strains: alternative to traditional transformation methods. Methods Enzymol. 350: 278–289.

Gibeaux, R., A. Z. Politi, F. Nedelec, C. Antony, and M. Knop, 2013 Spindle pole body-anchored Kar3 drives the nucleus along microtubules from another nucleus in preparation for nuclear fusion during yeast karyogamy. Genes Dev. 27: 335–349.

Golden, A., J. Liu, and O. Cohen-Fix, 2009 Inactivation of the C. elegans lipin homolog leads to ER disorganization and to defects in the breakdown and reassembly of the nuclear envelope. J. Cell Sci. 122: 1970–1978.

Gorjanacz, M., and I. W. Mattaj, 2009 Lipin is required for efficient breakdown of the nuclear envelope in Caenorhabditis elegans. J. Cell Sci. 122: 1963–1969.

Hatch, E. M., A. H. Fischer, T. J. Deerinck, and M. W. Hetzer, 2013 Catastrophic nuclear envelope collapse in cancer cell micronuclei. Cell 154: 47–60.

Heath, C. V., C. S. Copeland, D. C. Amberg, V. Del Priore, M. Snyder *et al.*, 1995 Nuclear pore complex clustering and nuclear accumulation of poly(A)+ RNA associated with mutation of the Saccharomyces cerevisiae RAT2/NUP120 gene. J. Cell Biol. 131: 1677–1697.

Holubcova, Z., M. Blayney, K. Elder, and M. Schuh, 2015 Human oocytes. Error-prone chromosome-mediated spindle assembly

favors chromosome segregation defects in human oocytes. Science 348: 1143–1147.
Hugerat, Y., F. Spencer, D. Zenvirth, and G. Simchen, 1994 A versatile method for efficient YAC transfer between any two strains. Genomics 22: 108–117.
Kao, F. T., and T. T. Puck, 1970 Genetics of somatic mammalian cells: linkage studies with human-Chinese hamster cell hybrids. Nature 228: 329–332.
Keith, K. C., and M. Fitzgerald-Hayes, 2000 CSE4 genetically interacts with the Saccharomyces cerevisiae centromere DNA elements CDE I and CDE II but not CDE III. Implications for the path of the centromere DNA around a cse4p variant nucleosome. Genetics 156: 973–981.
Kitamura, E., K. Tanaka, Y. Kitamura, and T. U. Tanaka, 2007 Kinetochore microtubule interaction during S phase in Saccharomyces cerevisiae. Genes Dev. 21: 3319–3330.
Kleylein-Sohn, J., J. Westendorf, M. Le Clech, R. Habedanck, Y. D. Stierhof *et al.*, 2007 Plk4-induced centriole biogenesis in human cells. Dev. Cell 13: 190–202.
Lebedev, I., 2011 Mosaic aneuploidy in early fetal losses. Cytogenet. Genome Res. 133: 169–183.
Liu, Y., S. Liang, and A. M. Tartakoff, 1996 Heat shock disassembles the nucleolus and inhibits nuclear protein import and poly (A)+ RNA export. EMBO J. 15: 6750–6757.
Loidl, J., 2003 Chromosomes of the budding yeast Saccharomyces cerevisiae. Int. Rev. Cytol. 222: 141–196.
Maiato, H., and E. Logarinho, 2014 Mitotic spindle multipolarity without centrosome amplification. Nat. Cell Biol. 16: 386–394.
Manandhar, G., H. Schatten, and P. Sutovsky, 2005 Centrosome reduction during gametogenesis and its significance. Biol. Reprod. 72: 2–13.
Mayer, W., A. Smith, R. Fundele, and T. Haaf, 2000 Spatial separation of parental genomes in preimplantation mouse embryos. J. Cell Biol. 148: 629–634.
McCoy, R. C., 2017 Mosaicism in preimplantation human embryos: when chromosomal abnormalities are the norm. Trends Genet. 33: 448–463.
McNally, A. K., and J. M. Anderson, 2011 Macrophage fusion and multinucleated giant cells of inflammation. Adv. Exp. Med. Biol. 713: 97–111.
Melloy, P., S. Shen, E. White, J. R. McIntosh, and M. D. Rose, 2007 Nuclear fusion during yeast mating occurs by a three-step pathway. J. Cell Biol. 179: 659–670.
Morales, L., and B. Dujon, 2012 Evolutionary role of interspecies hybridization and genetic exchanges in yeasts. Microbiol. Mol. Biol. Rev. 76: 721–739.
Muller, I., 1985 Parental age and the life-span of zygotes of Saccharomyces cerevisiae. Antonie van Leeuwenhoek 51: 1–10.
Nagaoka, S. I., T. J. Hassold, and P. A. Hunt, 2012 Human aneuploidy: mechanisms and new insights into an age-old problem. Nat. Rev. Genet. 13: 493–504.
Nam, H. J., R. M. Naylor, and J. M. van Deursen, 2015 Centrosome dynamics as a source of chromosomal instability. Trends Cell Biol. 25: 65–73.
Niepel, M., K. R. Molloy, R. Williams, J. C. Farr, A. C. Meinema *et al.*, 2013 The nuclear basket proteins Mlp1p and Mlp2p are part of a dynamic interactome including Esc1p and the proteasome. Mol. Biol. Cell 24: 3920–3938.
Nigg, E. A., and T. Stearns, 2011 The centrosome cycle: centriole biogenesis, duplication and inherent asymmetries. Nat. Cell Biol. 13: 1154–1160.
Nilsson-Tillgren, T., J. Petersen, S. Holmberg, and M. Kielland-Brandt, 1980 Transfer of chromosome III during kar mediated cytoduction in yeast. Carlsberg Res. Commun. 45: 113–117.
Quevedo, O., C. Ramos-Perez, T. D. Petes, and F. Machin, 2015 The transient inactivation of the master cell cycle phosphatase Cdc14 causes genomic instability in diploid cells of Saccharomyces cerevisiae. Genetics 200: 755–769.
Rahman, M. M., M. Munzig, K. Kaneshiro, B. Lee, S. Strome *et al.*, 2015 Caenorhabditis elegans polo-like kinase PLK-1 is required for merging parental genomes into a single nucleus. Mol. Biol. Cell 26: 4718–4735.
Rao, P. N., and R. T. Johnson, 1972 Premature chromosome condensation: a mechanism for the elimination of chromosomes in virus-fused cells. J. Cell Sci. 10: 495–513.
Rose, M. D., and G. R. Fink, 1987 KAR1, a gene required for function of both intranuclear and extranuclear microtubules in yeast. Cell 48: 1047–1060.
Ruddle, F. H., and R. S. Kucherlapati, 1974 Hybrid cells and human genes. Sci. Am. 231: 36–44.
Shen, S., C. E. Tobery, and M. D. Rose, 2009 Prm3p is a pheromone-induced peripheral nuclear envelope protein required for yeast nuclear fusion. Mol. Biol. Cell 20: 2438–2450.
Snape, K., S. Hanks, E. Ruark, P. Barros-Nunez, A. Elliott *et al.*, 2011 Mutations in CEP57 cause mosaic variegated aneuploidy syndrome. Nat. Genet. 43: 527–529.
Spang, A., I. Courtney, K. Grein, M. Matzner, and E. Schiebel, 1995 The Cdc31p-binding protein Kar1p is a component of the half bridge of the yeast spindle pole body. J. Cell Biol. 128: 863–877.
Tartakoff, A. M., and P. Jaiswal, 2009 Nuclear fusion and genome encounter during yeast zygote formation. Mol. Biol. Cell 20: 2932–2942.
Torres, E. M., T. Sokolsky, C. M. Tucker, L. Y. Chan, M. Boselli *et al.*, 2007 Effects of aneuploidy on cellular physiology and cell division in haploid yeast. Science 317: 916–924.
Vallen, E. A., M. A. Hiller, T. Y. Scherson, and M. D. Rose, 1992 Separate domains of KAR1 mediate distinct functions in mitosis and nuclear fusion. J. Cell Biol. 117: 1277–1287.
Vallen, E. A., W. Ho, M. Winey, and M. D. Rose, 1994 Genetic interactions between CDC31 and KAR1, two genes required for duplication of the microtubule organizing center in Saccharomyces cerevisiae. Genetics 137: 407–422.
Vanneste, E., T. Voet, C. Le Caignec, M. Ampe, P. Konings *et al.*, 2009 Chromosome instability is common in human cleavage-stage embryos. Nat. Med. 15: 577–583.
Vitre, B. D., and D. W. Cleveland, 2012 Centrosomes, chromosome instability (CIN) and aneuploidy. Curr. Opin. Cell Biol. 24: 809–815.
Walter, M. A., and P. N. Goodfellow, 1993 Radiation hybrids: irradiation and fusion gene transfer. Trends Genet. 9: 352–356.
Wickner, R. B., H. K. Edskes, F. Shewmaker, and T. Nakayashiki, 2007 Prions of fungi: inherited structures and biological roles. Nat. Rev. Microbiol. 5: 611–618.
Yuen, K. W., C. D. Warren, O. Chen, T. Kwok, P. Hieter *et al.*, 2007 Systematic genome instability screens in yeast and their potential relevance to cancer. Proc. Natl. Acad. Sci. USA 104: 3925–3930.
Zapanta Rinonos, S., J. Saks, J. Toska, C. L. Ni, and A. M. Tartakoff, 2012 Flow cytometry-based purification of S. cerevisiae zygotes. J. Vis. Exp. 67: e4197.

Communicating editor: O. Cohen-Fix